Numerical Study of Hydrogen enrichment and injector nozzle number impacts on non-premixed turbulent combustion characteristics in a Gas Turbine cannular Combustion Chamber

B.N. HAGANI [1], H. BOUSBAA [1], M. BENCHERIF [2]
[1] Mechanical Depertment, National Polytechnic school, LTE MA Oran, ALGERIA
[2] Mechanical Depertment, USTO, LTE-ENPO MA, ALGERIA

Abstract: - A numerical study on non-premixed combustion methane/air mixture, Hydrogen enrichment and injector nozzle number in swirl combustor is investigated using the Computational Fluid Dynamics CFD code. The method is based on the solution of Navier-Stokes unsteady equations using unstructured grid due to the complexity of geometry of the combustor. The turbulence modeling is carried out by RNG/k-ε) turbulence model. The H2 amount in the fuel mixture varies under constant volumetric fuel flow between 0 and 40% and the injector nozzle number is 4, 6 and 8. Results of this simulation show as the hydrogen rate increases, flame temperature, CO increases and CO2 decreases. On the other hand, the injector nozzle number minimizes the NOx and increases the CO level.

Key-Words: - Gas turbine, Combustion characteristics, hydrogen, nozzle number, non-premixed, emissions, numerical simulation.

Received: March 23, 2024. Revised: August 17, 2024. Accepted: September 21, 2024. Published: October 17, 2024.

1. Introduction

In recent years, industrial gas turbines have played an important role in power generation systems, such as nuclear power plants, power plants and hydrocarbon units, they are distinguished by their adaptation to simple cycles, combined or highly efficient cogeneration.

The power of a gas turbine is controlled by the heat input, which is generated by the combustion of the fuel/oxidant mixture in the combustion chamber one of the components of the gas turbine which has undergone several modifications and evolutions in order to improve the performance of these machines and also reduce the polluting gases generated at the end of the combustion reaction [1].

There are several types of combustion such as turbulent non-premixed combustion where there is the interaction between two phenomena, that of chemistry and the other of turbulence. Given the complexity of the combustion phenomenon, their experimental investigation poses a lot of questions, difficulties, so this approach remains expensive and limited to certain operating conditions, however, numerical calculation may constitute the most suitable solution given the progress made in the field of computing and modeling [2].

Several numerical and experiment studies on the combustion in chamber of gaz turbine have been which showed that the combustion is influenced by several parameters such as oxygen or hydrogen enriched and velocities admission. The combustion of methane-air mixture and oxygen enriched in gas turbine combustion chamber was experimented numerically by different studies: Habib et al. [3] studied experimentaly the atmospheric diffusion oxy-fuel combustion flame in a gas turbine combustor alimented with CH_4 and a mixture of CO_2 and O2. in this study different operating parameters are considered as equivalence ratio (0.5–1), ratio of mixture O2/CO2. The objectif of the study focus to the percentages of O2 to get a stable flame and the meseare of flame and exhaust gas temperatures in combustion chamber. The results indicate the flame is very stable at the mixture ratio of 0.65 and flue gas temperatures are reduced with the increase of the equivalence ratio. Zhang et al. [4] studied the the effects natural gas combustion under different oxygen concentrations on flame characteristics NO production and flame kinetics. the results indicate, With the addition of oxygen, the flame temperature, the heat release rate and NO emission are increased. On the contrary, and the flame thickness decreases. Xu et al. [5] stidies numerically the effect of oxygen concentrations (19.5-36%) and velocities admission (47.16-261.18 m/s) on combustion and NO emission. Overall, the results show that the non-premixed air/oxygen combustion can provide low NO emission if combustion air with low oxygen contents is employed, while for highly oxygen-enriched concentration, the together adition oxygen with high velocity is suggested. Hussein and Salih [6] studied

numerically, the effect of the oxygen ratio for methane–air combustion and compared with experiment study. From the results, its clear that was an improvement in the combustion with the increasing in oxygen ratio.

For the combustion of methane-air mixture and hydrogen enriched in gas turbine combustion chamber was experimented numerically by different studies: Gregory et al [7] studied numericallycarried out by on the influence of hydrogen addition on the response of the methane lean premixed flame, where they found that it increases the flame speed and therefore subsequently its maximum stretch rate that causes extinction.

Cozzi and Coghe [8] studied the influence of natural gas mixed with hydrogen fuel n the non-premixed burner. The results showed that adding hydrogen, the soot, CO and NOx emissions increased.Park et al. [9] studied the effect of hydrogen addition (0–30%) in the methane/air lean-premixed flame. The analysis showed that the doping of hydrogen to methane/air mixtures will increase the flame temperature also NO concentration.

Shin and Cho [10] studies the effect of Hydrogen enrichement on temperature, flame speed and emissions (NOx, CO) using CHEMKIN-Pro with GRI 3.0 detailed chemistry in gas turbine fuelled with GNL (Gas Naturan Liquid). The results indicate the increase of flame temperature and the flame speed. However, addition of Hydrogen reduces CO emissions and increases NOx emissions. Pignatelli et al. [11] studied numerically the impact of pilot flame, Reynolds number and hydrogen-enriched methane on the performance and emissions in dry-low-emission (DLE) burner-based gas turbine engines. From the results, its clear the Reynolds number the positive impact on the pilot flame and the NOx and CO emissions decrease lower with increasing hydrogen ratio.Zhang et al. [12] studied numerically the effect of hydrogen addition (0–75%) for analyzing the effects of blended fuel and thermal boundaries on the combustor thermal environment on a dry-low-emission combustor. The results show that when the fuel hydrogen volume percentage increases, the maximum gas temperature and H2O concentration on the central axis of the combustor increase.

In the present work we will study in the first time the effect of mixture CH_4/H2 at different fractions in non-premixed turbulent combustion chamber, also the influence of introducing a quantity of air as dilution air on the shape and temperature of the flame and therefore the emissions of NOx and CO. In the second time, the impacts of injector nozzle number in combustion and emissons characteristics in a Gas Turbine cannular Combustion Chamber, where the design of the latter was carried out by the Solidworks design software and the numerical simulation by the ANSYS CFX16.2 software.

2. Numerical model setup

2.1 Governing equations:

Any modeling problem in combustion is based on the equations of aerothermochemistry, a system comprising the conservation equations of chemical species, mass, momentum, energy and the equation of state given as follows [13]:

- ***Continuity equation for species m :***

$$\frac{\partial \rho_m}{\partial t} + \frac{\partial \rho_m u_j}{\partial x_j} = \frac{\partial}{\partial x_j}\left(\rho D \frac{Y_m}{\partial x_j}\right) + S_m \quad (1)$$

With : $Y_m = \frac{M_m}{M_{tot}} = \frac{\rho_m}{\rho}$

- ***Total mass equation :***

$$\frac{\partial \rho}{\partial t} + \frac{\partial \rho\, u_i}{\partial x_i} = S \quad (2)$$

- ***Momentum equation for the fluid mixture:***

$$\frac{\partial \rho u_i}{\partial t} + \frac{\partial \rho u_i u_j}{\partial x_j} = -\frac{\partial P}{\partial x_i} + \frac{\partial \sigma_{ij}}{\partial x_j} + S_i \quad (3)$$

Where the viscous stress tensor is defined by:

$$\sigma_{ij} = \mu\left(\frac{\partial u_i}{\partial x_j} + \frac{\partial u_j}{\partial x_i}\right) + \left(\mu' - \frac{2}{3}\mu\right)\left(\frac{\partial u_k}{\partial x_k}\delta_{ij}\right)$$

Where, u is fluid velocity, ρ is density, Si is source term, P is fluid pressure, μ is viscosity, μ' expansion viscosity (set to zero), δij is Kronecker delta.

With:

$$\delta_{ij} = \begin{cases} 1 & if \quad i = j \\ 0 & if \quad i \neq j \end{cases}$$

- ***Internal energy equation:***

$$\frac{\partial \rho E}{\partial t} + \frac{\partial \rho u_j E}{\partial x_j} = -P\frac{\partial u_j}{\partial x_j} + \sigma_{ij}\frac{\partial u_i}{\partial x_j} + \frac{\partial}{\partial x_j}\left(K\frac{\partial T}{\partial x_j} + \rho D \sum_m h_m \frac{\partial Y_m}{\partial x_j}\right) + \dot{Q}^s + \dot{Q}^c \quad (4)$$

Where$\dot{Q}^s$ and $\dot{Q}^c$are terms due to spray interactions and chemical heat, respectively.

The transport coefficients are given by the following relations:

$$D = \frac{\mu}{\rho S_c} \text{ and } K = \frac{\mu C_p}{P_r}$$

The air-fuel mixture introduced inside the cylinder is assumed to be an ideal gas whose behavior equations are:

$$p = R_0 T \sum_m \left(\frac{\rho}{M_m}\right) \quad (5)$$

$$E(T) = \sum_m \left(\frac{\rho_m}{\rho}\right) E_m(T) \quad (6)$$

$$C_p(T) = \sum_m \left(\frac{\rho_m}{\rho}\right) C_{pm}(T) \quad (7)$$

$$h_m(T) = E_m(T) + R_0 \frac{T}{M_m} \quad (8)$$

2.2 Turbulence model

In this study, the determination of the residual stress terms in the governing equations was carried out by applying the *RNGk-ε* turbulence model as a closure technique.

The standard *RNG K-ε* turbulence model is a modeling approach that stems from the unsteady Navier-stockes equations using a mathematical technique called Re-normalization-Group. This improved model incorporates a modification in the dissipation equation "***ε***" to better account for turbulent characteristics at finer scales [14].

The turbulent kinetic energy and dissipation equations of the model are as follows:

- Kinetic energy equation:

$$\frac{\partial(\rho k)}{\partial t} + \frac{\partial(\rho k\, U_j)}{\partial x_j} = \frac{\partial}{\partial x_j}\left(\alpha_k \mu_{eff} \frac{\partial k}{\partial x_j}\right) + G_k - \rho\varepsilon \quad (9)$$

- Dissipation rate equation:

$$\frac{\partial(\rho\varepsilon)}{\partial t} + \frac{\partial(\rho\varepsilon\, U_j)}{\partial x_j} = \frac{\partial}{\partial x_j}\left(\alpha_\varepsilon \mu_{eff} \frac{\partial \varepsilon}{\partial x_j}\right) + C_{1\varepsilon}\frac{\varepsilon}{k} G_k - C_{2\varepsilon}\rho\frac{\varepsilon^2}{k} R_\varepsilon \quad (10)$$

G_k; Represents the production of turbulent kinetic energy due to the average speed gradient

$C_{1\varepsilon}$and , $C_{2\varepsilon}$: are constants.

α_k and α_ε are the inverses of the effective Prandtl numbers for k and ε respectively.

2.3 Combustion model

In our study, the Probability Density Function (PDF) Flamelet model has been selected for modeling non-premixed combustion.

The term flamelets defines a one-dimensional thin reactive-diffusive layer embedded in a non-reactive turbulent flow.

The turbulent diffusion flame can be seen as a collection of flat laminar flames stretched by turbulence, but whose internal structure remains little modified. This vision, introduced by Peters and Kouznetsovo then widely discussed by [15, 16], makes it possible to simplify the modeling of the Chemistry Turbulence interaction. The resolution method therefore boils down to knowledge of the relationships that exist between chemistry and the independent parameters on which it depends (Z, χ) and their statistical distribution. For each species i, the average mass fraction is written:

$$\tilde{Y}_i(x_i, t) = \int_0^1 \int_0^\infty Y_i(Z, \chi, t)\, P(Z, \chi; x, t) dZ d\chi \quad (11)$$

With;

$$Z = \frac{1}{1 + \emptyset}\left(\emptyset \frac{Y_F}{Y_F^\infty} - \frac{Y_0}{Y_0^\infty} + 1\right)$$

Or :

Y_F^∞: designates the mass fraction of fuel in the fuel flow.

Y_0^∞: designates the mass fraction of oxidant in the oxidant flow.

Φ: denotes wealth

And χ: scalar dissipation; which is a structural characteristic of diffusion flames.

3. Combustor geometry description and simulation details

The basic combustor geometry (the injector and the flame tube) of the Cannular type gas turbine is shown in the figure below. The combustion chamber size is 777.89 mm in Z direction, 300mm in Y direction and 230mm in X direction.

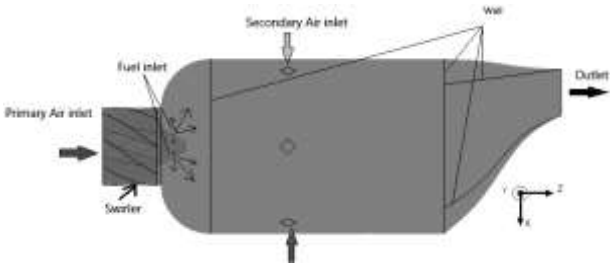

Fig. 1 Solid model of combustor flow domain

The inlet primary air is guided by 8 vanes to give the air a vortex velocity component, the total area of the main primary air inlet is 57 cm^2. Fuel is injected through six fuel inlets into the swirling primary air stream, each with an area of 0.14 cm^2. Secondary air is injected into the combustion chamber through four side air inlets, each with an area of 2 cm^2.

Following the study, the combustion chamber is considered as a single control volume whose nature is chosen as fluid to avoid the study at the edge of the walls and therefore focus only on the flow inside the burning.

3.1 The mesh

The geometric complexity of the configuration studied prompted us to use an irregular mesh because the flame can during the calculation be located in any area of the chamber as well as the unstructured mesh minimizes the dissipation of the numerical schemes.

The mesh used is of the tetrahedral type in all the calculation domain, it contains approximately 27948 nodes and 138351 elements with the areas where we are interested in seeing the results such as the injection areas and the dilution air inlet are meshed finer with a mesh size of 5 mm and the rest of the geometry with a mesh size of 10 mm, the mesh geometry is shown in fig.2 below.

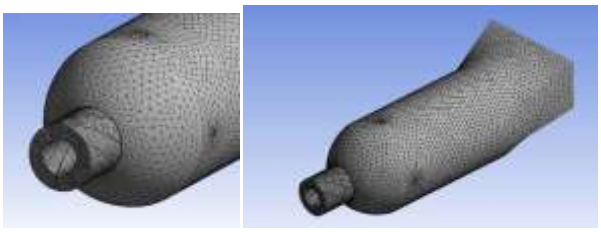

Fig. 2 Mesh geometry of gas turbine can combustor

3.2 Simulation details

To close the aerothermochemical equations system cited above, the *RNG k-ε* model was chosen to model turbulence for its robustness and its good ability to model free shear flows.

Also for the modeling of the non-premixed combustion of methane, the FLAMLET PDF model was chosen assuming that the combustion occurs in thin sheets with an internal structure called a flamelet, the turbulent flame in our case is then treated as a set of flamelets. integrated in the flow field, also the information on the laminar model is pre-calculated and stored in a library to reduce the calculation time (PDF table).

To simulate NOx emissions, the Zeldovitch model is selected; thus the finite volume method and second-order upwind are used to solve the Naiver-Stokes equations acting on the flow.

The convergence criteria are 10^{-4} for mass, momentum, kinetic energy and dissipation rate and even species conservation equations, for energy equations and pollutants the convergence criterion is the order of 10^{-6}.

3.3 Boundary conditions

The table below summarizes the boundary conditions taken for our study:

Primary air	▪ Flow regime: Subsonic; ▪ The injection velocity:10 m/s ▪ Heat transfer: Static temperature T= 298 K ▪ The turbulence intensity: 10%; ▪ Mass fraction of oxygen :Y_{O2}= 0.23 ▪ Mass fraction of Nitrogen :Y_{N2}= 0.77
Fuel	▪ Flow regime: Subsonic; ▪ The injection velocity: 45 m/s ▪ The injector diameter: 1 mm ▪ The temperature: T= 300 K; ▪ The turbulence intensity: 10%; ▪ Thermal radiation: Local temperature.
Secondary air	▪ The injection velocity:6 m/s ▪ The temperature: T= 298 K; ▪ The turbulence intensity: 10%;
	▪ Mass fraction of oxygen: Y_{O2}= 0.232.
Wall	▪ Wall heat transfer was adiabatic; ▪ Wall boundary condition was no slip. ▪ Wall roughness was Smooth.

4. Results and discussion

4.1 Aerodynamics characteristics

In order to validate the geometry, a non-reactive flow is studied whose injected fluid is only air at 289 K and 1.013 atm. The figures below show the evolution of the streamlines along the geometry and the velocity fields for the non-reactive case:

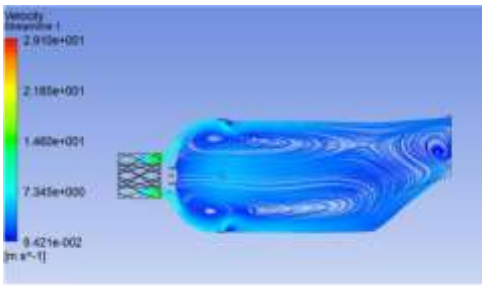

Fig. 3: Streamlines (non-reactive case)

From Fig. 3, there are recirculation zones created in the corners of the chamber due to the sudden widening;these are the corner recirculation zones "CRZ", these zones have a very important role, they promote the attachment of the flame.

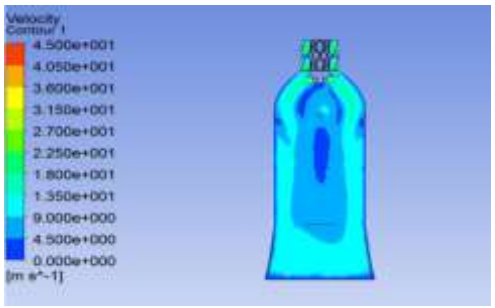

Fig. 4 : Velocity fields along the CC (non-reactive case)

According to Fig.4; we see that the speed in the combustion chamber is well distributed from the moment of injection until the exhaust of the combustion products. From these results we can validate the aerodynamics of the geometry and exploit it in the rest of our study.

4.2 Combustion evolution of Methane

This second case corresponds to a reactive flow, with injection of CH_4 fuel. The Fig. 5 below shows

the current line which manifests itself along the combustion chamber after fuel injection and the start of combustion, the color code presented on the left of the figure represents the values of the speed axial.
In the primary zone, the low axial velocities at the center of the combustion chamber indicate the existence of an internal recirculation zone. The swirl vanes around the fuel nozzle generate a strong swirling flow in the combustion air inside the combustion chamber.

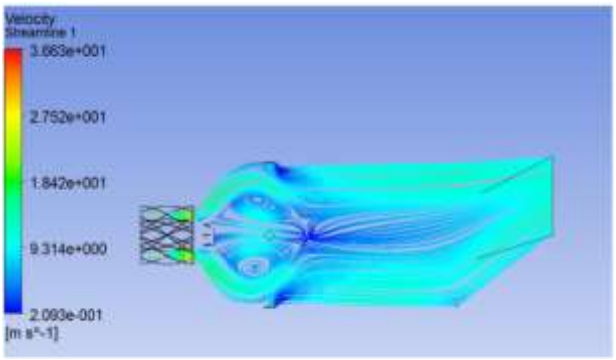

Fig. 5 : Velocity streamline in meridian plan (OYZ)

Fig. 6; represents the contour of the temperature in the combustion chamber, we notice that the flame temperature increases along the combustion chamber, the maximum combustion temperature is very high, it reaches a value of 2211 K, with a core offlame of a lower temperature than the flame front which is at a temperature of about 1500 K, so the flame is well stretched.

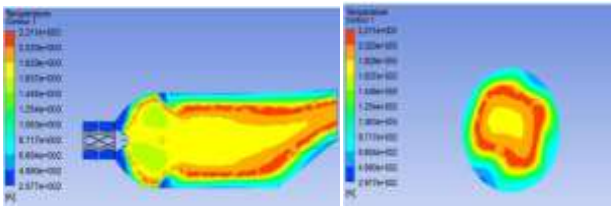
Fig. 6: Temperature distribution along the chamber

The velocity distribution along the combustion chamber is shown below in fig.7; where it is noted that the speed in the combustion chamber decreases by the methane injection speed which is of the order of 45 m/s at the exit of the chamber (the exhaust) is this from the point where the mixture Air/Methane is created and therefore the start of the reaction between them (start of combustion).

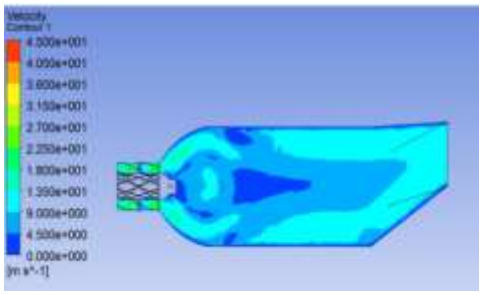
Fig. 7 : Velocity distribution along the chamber

The figures below represent the axial distribution of the different species such as CH_4, O_2, CO, NO and NO_2 along the combustion chamber:

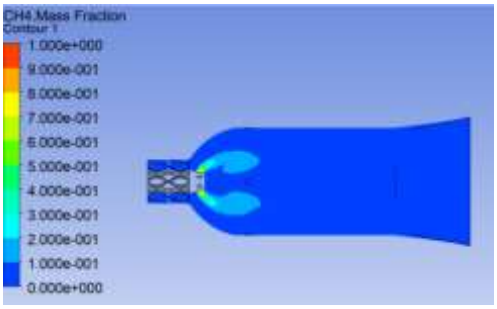

Fig. 8 : Distribution of CH_4 along the combustion chamber

Fig.8 shows the axial distribution of CH_4 at the start of its injection, there is a concentration of the latter at the outlet of the injector which begins to weaken with the formation of the CH_4/Air mixture.

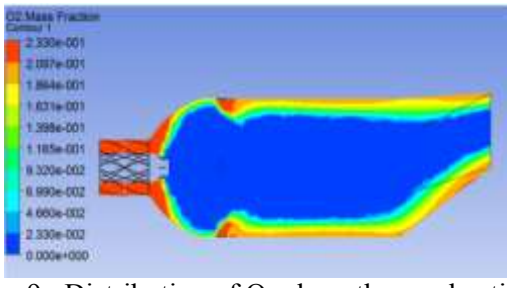
Fig. 9 : Distribution of O_2 along the combustion chamber

The axial distribution of O_2 is shown in figure Fig. 9, where there is a concentration of this species in the injection zone of the two primary and secondary airs and decreases from the zone where combustion takes place.

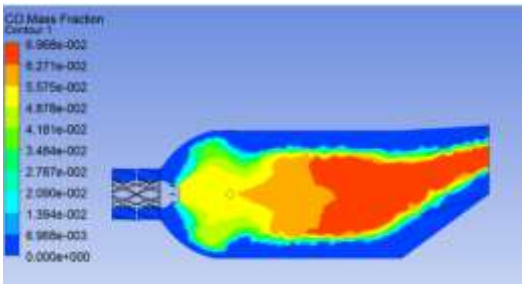

Fig. 10 : Axial distribution of CO

Fig.10; shows the variation of CO along the combustion chamber, according to this figure we observe a variation of the mass fraction of CO inversely proportional to the flame temperature; therefore the zones where the flame temperature is high we observe a low concentration of CO and the reverse for the zones where the flame temperature is low.

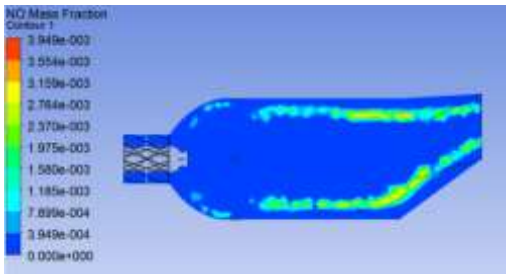

Fig. 11 : Axial distribution of NO

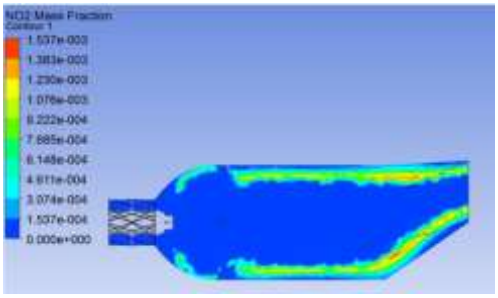

Fig. 12 : Axial distribution of NO_2

The main nitrogen oxides NOx produced during combustion are nitrogen monoxides NO and nitrogen dioxides NO_2, the axial distribution of these two species is shown in Fig. 11 and Fig. 12 respectively.

It can be seen that above 1825 K, there will be an increase in the production of NOx, especially thermal NOx. The level of NOx emissions from a combustion chamber depends on the interaction between physical and chemical processes and is strongly dependent on temperature.

4.3 Impact of mixture CH_4/H_2

In this part we will study the effect of hydrogen injection on the structure of the methane diffusion flame and the products generated by the latter.

The same boundary conditions of the previous study will be used to examine the effect of injecting hydrogen into the central methane jet to fuel the combustion for different percentage mixtures of CH_4 and H_2.

The cases studied are summarized in the table below:

The fuel	% CH_4	% H_2
Methane	100	0
Mixture N°1	80	20
Mixture N°2	70	30
MixtureN°3	60	40

Table. 1 : CH_4-H_2 mixtures

The temperature distribution for the four chosen fuel configurations with these hydrogen doping (0, 20%, 30% and 40%) are shown in figures (13, a-d) respectively.

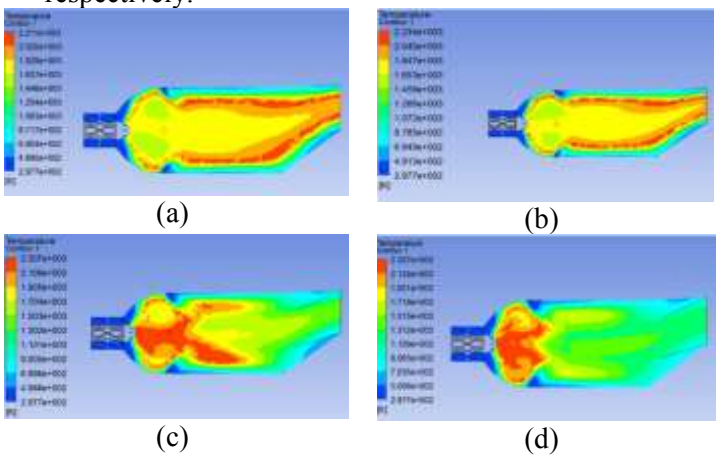

(a) (b)

(c) (d)

Fig. 13: Temperature distribution along the chamber for the four fuels

According to the results presented by the figures above for the distribution of the temperature with different fuels where the doping of hydrogen is different, it is clearly noticed that the flame temperature increases with the increase in the quantities of hydrogen injected. The shape of the diffusion flame changes with the amount of hydrogen injected where we see that the stretch of the flame decreases with the increase in the amount of hydrogen injected into the chamber, so it is shorter for the case of 40% hydrogen and 60% Methane.

- **CO distribution**

The figures (14, a-d) show the variation of CO along the combustion chamber for the four chosen fuel configurations with these doping hydrogenated (0, 20%, 30% and 40%) respectively.

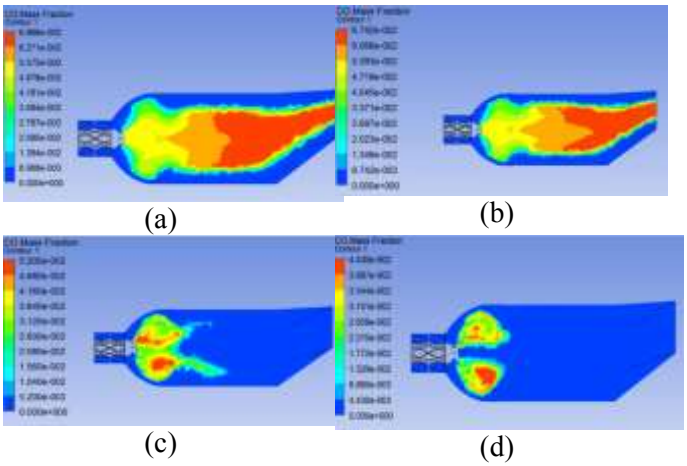

(a) (b)

(c) (d)

Fig. 14 : Distribution of CO for the four fuels

According to the results shown in the figures (14, a-d), it can be seen that the addition of hydrogen has a positive influence on the emissions of the CO where we note that the addition of hydrogen decreases the production of CO; for 40% of hydrogen injected we have only 0.004403 as mass fraction of CO while for 0% of hydrogen we have 0.006968 of CO (mass fraction).

- **CO_2 distribution**

The figures (15, a-d) show the variation of CO_2 along the combustion chamber for the four chosen fuel configurations with these doping hydrogenated (0, 20%, 30% and 40%) respectively.

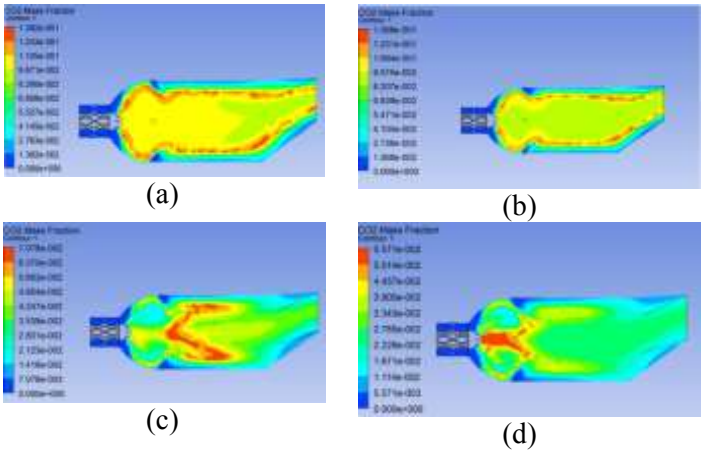

(a) (b)

(c) (d)

Fig. 15 : Distribution of CO_2 for the four fuels

According to the results of the simulation shown in the figures above, we have been able to observe the effect of hydrogen injection with different concentrations on CO_2 emissions, where we have an inversely proportional relationship between the addition of hydrogen and the amount of CO_2 produced by combustion; we have for 0% of hydrogen a mass fraction of CO_2 of order of 0.1382 whereas for 40% of hydrogen only 0.005571 of CO_2; therefore, a 50% reduction in CO_2 emissions.

4.4 Impact of the injector nozzle number

In this part of our study we will study the influence of the number of fuel injection pores (located in front of the injector), for this the same boundary conditions (of temperature, injection speeds and pressure), the turbulence model, the combustion model as well as the convergence criteria as the previous part, except that the geometry and the mesh change in this part.

The geometries used in this part are shown in the figures (16, a-c) with 4, 6 and 8 pores respectively.

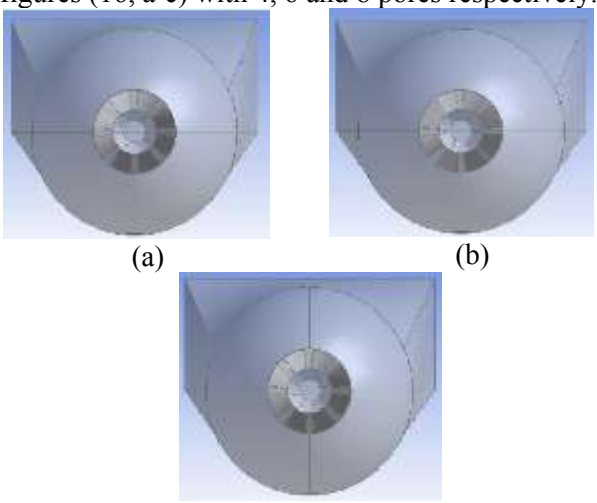

(a) (b)

(c)

Fig. 4 : The geometries used

- ***The mesh:*** The 3-D modeling of the combustor and deferent nozzles has been done using the pre-processors ANSYS CFD (Fig. 17) . the table 2 present the variation of nodes and elements numbers with nozzles number.

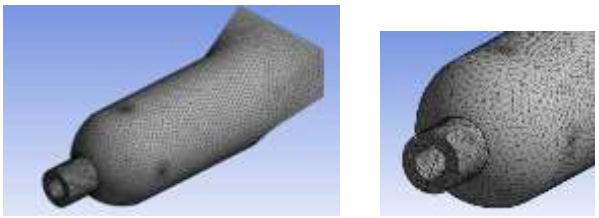

Fig. 5 :The mesh

The combustion chamber	Number of nodes	Number of elements
With 4 nozzles	26948	133394
With 6 nozzles	27948	138351
With 8 nozzles	27119	134395

Table. 2 : Mesh statistics

▪ ***The streamlines for the three injector nozzle configurations:*** Figures (18, a-c) show the streamlines created in the combustion chamber for the injector configuration with 4, 6 and 8 pores respectively.

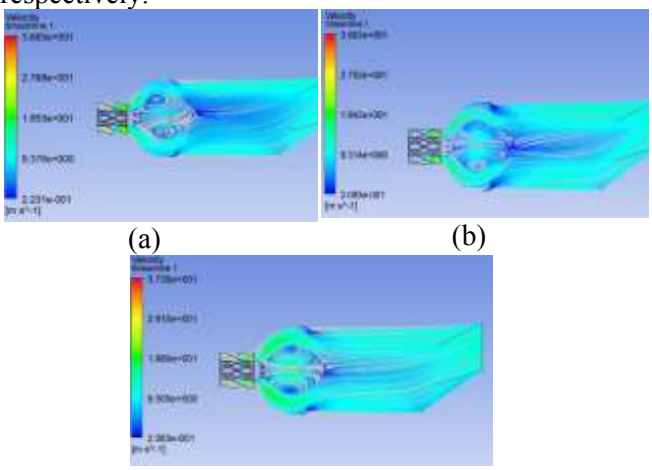

(a) (b)

(c)

Fig. 18 : The streamlines for the three injector configurations

According to Fig. 18, we note that the lines of currents for the three configurations are different, where we have for the injector with 8 pores a high speed compared to the two others, as we also note for the internal recirculation zones which are responsible for the stability of flame and burning intensity are well structure with high pore count.

▪ ***The temperature field for the three injector nozzle configurations:*** In the figures (19, a-c) the temperature distribution for the injector configuration with 4, 6 and 8 pore is shown respectively.

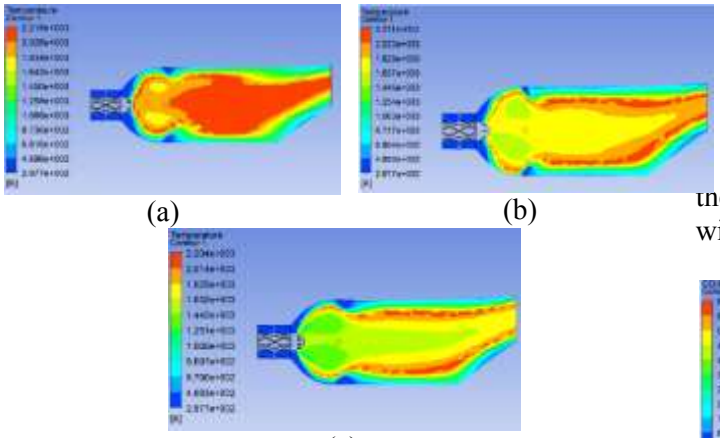

(a) (b)

(c)

Fig. 19 : Temperature distribution for the three injector configurations

From the figures above, it can be seen that the number of injection pores influences the shape of the Methane flame and also its temperature; where we clearly see that the temperature is high for the case where only 4 injection pores were used, while it begins to decrease by increasing the number of pores.

So by increasing the number of injection pores, the flame temperature decreases and its shape becomes more stable for the correct distribution of the fuel, and this allows us to control the emissions generated by combustion as we will see later.

▪ ***The distribution of NO_2:*** Figures (20, a-c) show that the formation of nitrogen oxides NOx more precisely NO_2 is mainly a function of the flame temperature of the fuel, the rate of formation of NOx increases exponentially as the temperature increases.

So our case where we played on the number of pores of the injector we see that the increase in pores decreases the flame temperature and this led to a decrease in the production of NO_2.

There was a decrease in NO_2 from the mass fraction of 1.566×10^{-3} with a 4 pores injector to a mass fraction of order 1.516×10^{-3} with an 8 pores injector.

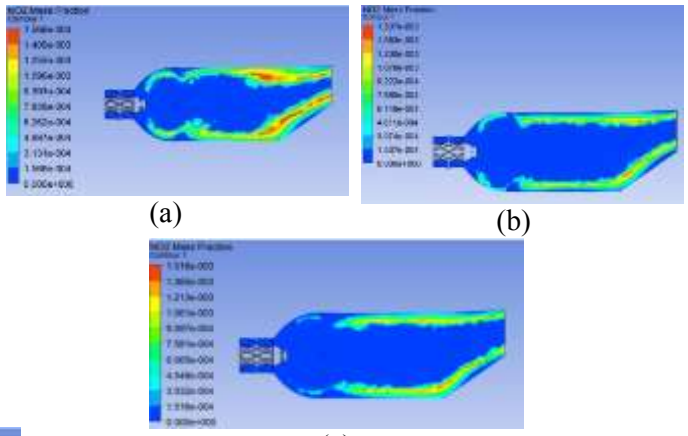

(a) (b)

(c)

Fig. 20 : The distribution of NO_2 for the three injector configurations

The distribution of CO: In figures (21, a-c) the CO distribution for the injector configuration with 4, 6 and 8 pore is shown respectively.

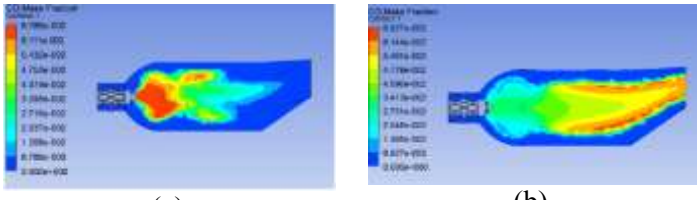

(a) (b)

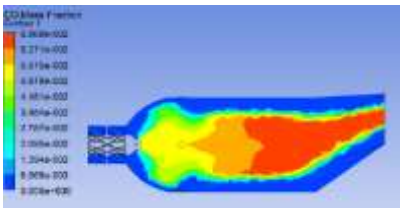

(c)

Fig. 21 : The CO distribution for the three injector configurations

According to the results shown in the figure (21, a-c), we notice that the variation of the numbers of injection pores influences the formation of CO, we see that by increasing the number of injection nozzle from 4 to 8 pores led to an increase in the mass fractions of this species from a value of 6.789×10^{-2} for a 4 pore injector to 6.968×10^{-2} for an 8 pore injector.

5. Conclusion

This work aims to improve the knowledge and understanding of the phenomena involved in a non-premixed turbulent combustion process of Methane, using the ANSYS CFD 16.2 code. Our first goal was to characterize the behavior and the different phenomena involved during the non-premixed combustion of Methane, the temperature point and the emissions.The other objective of this work was to characterize the addition of hydrogen on the turbulent combustion Methane / air.

- In a first calculation, we considered the air flow in the combustion chamber so the case without flame, this allowed us to understand the aerodynamic behavior of the geometry studied and therefore continue our study.
- After the aerodynamic study, the reactive case was studied where we could see the streamlines, the speed and temperature contours and finally the mass fractions of species present in the combustion chamber such as CH_4, CO, CO_2, NO and NO_2.
- In the second part of our work, the study of the influence of the addition of Hydrogen at different concentrations to the non-premixed flame of Methane was made; where we characterized the evolution of the flame temperature as well as the emissions produced by this reaction, we found that the temperature of the flame increases with the increase in the doping by H_2 this essentially reduces the CO_2 but we had a slight increase in CO.
- In the third part of our work, we will study the influence of the number of fuel injection nozzle, its clear that the NOx decreased and the CO increased with number of nuzzle.
- In order to give good results it is necessary to make a combination between the two techniques.

References

[1] Boukens Mohamed Walid et GuennounSefiane; “Etude thermodynamique de la turbine à gaz type MAN THM 1304, ” Dissertation presented for obtaining the master's degree; 2019.

[2] Zakaria Hallas; “Modélisation numérique d’une flamme turbulente pré-mélangée du méthane-air enrichie par lhydrogène avec le modelé EDM,” ; Dissertation presented for obtaining the master'sdegree ; 2011.

[3] HABIB, MOHAMED A., NEMITALLAH, MEDHAT A., AHMED, PERVEZ., SHARQAWY, MOSTAFA H., BADR, HASSAN M., MUHAMMAD, INAM., YAQUB, MOHAMED., “EXPERIMENTAL ANALYSIS OF OXYGEN-METHANE COMBUSTION INSIDE A GAS TURBINE REACTOR UNDER VARIOUS OPERATING CONDITIONS,” ENERGY, VOL 86, PP 105-114, 2015.

[4] Zhang, K., Hu, G., Liao, S., Zuo, Z., Li, H., Cheng, Q., Xiang, C. “Numerical study on the effects of oxygen enrichment on methane/air flames,” Fuel, 176: pp93-101, 2016. https://doi.org/10.1016/j.fuel.2016.02.064

[5] Xu, S., Xie, Y., Huang, P., Ren, H., Tu, Y., Liu, H. “Non-premixed air/oxygen jet burner to improve moderate or intense low-oxygen dilution combustion characteristics in oxygen-enriched conditions,” Energy & Fuels, 35(11): 9609-9622, 2021.
https://doi.org/10.1021/acs.energyfuels.1c00656

[6] Hussein M, Salih Adel H. Ayaal, “Enhancement of Methane-Air Combustion with Increasing Oxygen Ratio,” 40(1), pp. 353-358, 2022. DOI: https://doi.org/10.18280/ijht.400143.

[7] Gregory S. Jackson , Roxanne Sai, JosephM. Plaia, Christoph er M. Boggs, Kenneth T. Kiger ; “Influence of H2 on the response of lean premixed CH4 flames to high strained flows,” ; Combustion and FlameVolume 132, Issue 3, Pages 503-511, 2003.

[8] Cozzi, F.; Coghe, A. “Behavior of hydrogen-enriched non-premixed swirled natural gas flames. Int. J. Hydrogen Energy , 31, 669–677, 2006.

[9] SUNGWOO PARK, “HYDROGEN ADDITION EFFECT ON NO FORMATION IN METHANE/AIR LEAN-PREMIXED FLAMES AT ELEVATED PRESSURE,” INTERNATIONAL ASSOCIATION FOR HYDROGEN ENERGY, VOL 46, ISSUE 50, 21, PP 25712-25, 2021.

[10] Youngjun Shin, Eun-Seong Cho, “Numerical Study on H2 Enriched NG Lean Premixed

Combustion," Journal ofKorean Society Combustion, Vol26 (1), 2021.
[11]F. Pignatelli , H. Kim , A.A. Subash , X. Liu , R .Z. Szasz , X.S. Bai , C. Brackmann , M. Aldén , D. Lörstad,"Pilot impact on turbulent premixed methane/air and hydrogen-enriched methane/air flames in a laboratory-scale gas turbine model combustor," International Journal of Hydrogen Energy, Vol 47, Issue 60, PP 25404-25417, 2022.
[12] XIAOXIN ZHANG, QING AI, WENZHUO WANG, "EFFECTS OF HYDROGEN/METHANE ON THE THERMAL ENVIRONMENT OF HEAVY-DUTY GAS TURBINE COMBUSTOR," AMERICAN INSTITUTE OF AERONAUTICS AND ASTRONAUTICS, 2023. HTTPS://DOI.ORG/10.2514/1.T6798
[13] ANSYS, Inc. ANSYS CFX16.2: User's Guide; Theory Guide; UDF Manual, 2016.
[14] Vincent Robin, "Contribution à la modélisation des écoulements turbulents réactifs partiellement pré-mélangés," ; thèse pour l'obtention du grade de docteur de l'université de Poitiers ; 2006.
[15] D.C. Haworth, "Progress in probability density function methods for turbulent reacting flows," Progress in Energy and Combustion Science 36, PP168–259, 2010.
[16] Lotfi Ziani, AblaChaker, Khaled Chetehouna, Malek Ali ; "Numerical simulations of non-premixed turbulent combustion of CH4–H2 mixtures using the PDF approach,"; International Journal of Hydrogen Energy 38(20):8597–8603, 2013.

Contribution of Individual Authors to the Creation of a Scientific Article (Ghostwriting Policy)

The authors equally contributed in the present research, at all stages from the formulation of the problem to the final findings and solution.

Sources of Funding for Research Presented in a Scientific Article or Scientific Article Itself

No funding was received for conducting this study.

Conflict of Interest

The authors have no conflicts of interest to declare that are relevant to the content of this article.